Suitability of Sb-doped SnS thin films for PV applications, synthesized chemically

Kesava Vamsi Krishna V.[a] A. Thirupathi[b], A. Gurusampath Kumar[b], Ravindharan Ethiraj[c,*]

[a]*Research Scholar, Department of Physics, Rayalaseema University, Kurnool*
[b]*Dept. of Physics, Malla Reddy Engineering College, Secunderabad*
[c]*Dept. of Physics, Osmania University*
* Corresponding author: mrecphysics@gmail.com

Abstract:

In the recent times, SnS thin films drew much attention for obvious reasons like abundancy, and lesser toxic nature. Researchers across the world proved the suitability of SnS thin films for Photovoltaic (PV) applications, as absorber layer in a solar cell. In this paper, an attempt is made to establish the suitability of Antimony (Sb) – doped SnS thin films for Photovoltaic applications. Chemical Bath Deposition (CBD) method was used to deposit the undoped and Antimony doped SnS thin films. The properties like structural, optical, and electrical were studied besides studying the composition of the grown films. The crystallinity of the deposited films showed an improving trend with the Sb-doping concentration till 5 atomic percentage. The optical band gap showed variation between 1.147 eV to 1.25 eV. The electrical resistivity and the charge carrier concentration marked opposite trends with the former decreasing significantly while the latter increased with the Sb-doping concentration. Electrical resistivity as low as 2.72 x 10^{-2} ohm-cm and carrier concentration as high as 3.65 x 10^{19} cm $^{-3}$ were exhibited by 5 atomic % Sb doped SnS films.

DOI: 10.48047/ecb/2023.12.Si8.760

1. Introduction:

Lesser toxicity, earth abundance, apt band gap, higher absorption coefficient and apposite efficient conversion coinciding with the theoretical value of >25% made SnS a dependable alternative for absorber layers in thin film solar cells, replacing the highly toxic CdTe and CIGS PV absorbers [1,2]. SnS thin film solar cells with efficiency as low as of about 4.36% was recorded till the recent times, in comparison to the expected theoretical efficiency [3]. Bulk material defects, improper crystallinity, resistivity, and morphology with tinier grains of SnS thin film etc were identified as the contributing factors for the lower efficiency of the SnS thin film solar cell. More importantly, the band discontinuities in SnS heterojunction confine the performance of the solar cells made of SnS. The carrier transport via the junction is curbed by the energy spikes in the conduction band that resulted due to the band discontinuities. In addition, the interface recombination that enables the negative conduction band discontinuity creation, also minimizes the efficiency of SnS {4-6]. Doping SnS with an appropriate element can not only modify the band gap but can further possibly turn the negative conduction band into positive [7]. Even the valence band discontinuity can be addressed with doping. The acceptor density and the resistivity can significantly be changed by doping at the Antimony vacant sites. By suitably restricting the doping concentration, the required density of 10^{15} – 10^{19} cm^{-3} can easily be achieved, in order to enhance the solar cell performance. Therefore, it

poses an unavoidable need to optimize the doping concentration to obtain the required acceptor density in SnS thin films.

Doping with In [8,9], Pb [10], Al [11], Bi [12] and Ag [13-16], has encouragingly changed the opto-electrical properties of SnS. The present authors selected to verify the suitability of Antimony (Sb) as a potential dopant for enhancing the charge carrier concentration in SnS.

Numerous deposition techniques were used to deposit doped SnS thin films which include techniques like atomic layer deposition [18], thermal evaporation [13], two-step process [17], pulse electro deposition [19], chemical bath deposition (CBD) [15], spray pyrolysis [14]. Among these different techniques, CBD was identified as cost effective and relatively simple method. This paper presents the synthesis of Sb doped SnS thin films by CBD intended for solar cell applications, along with the characterization of these films.

2. Experimental details:

2.1 Materials and procedure:

A reliable, economical and relatively simple deposition technique called CBD was used to deposit the pristine and Antimony doped SnS thin films. Equation (1) mentioned below was used to determine the Sb-doping concentration which was fixed at 1%, 3% and 5% in the present study [20].

$$\text{Sb-doping concentration (at\%)} = \frac{[Sb]_{Sol}}{[Sn]_{Sol}} \quad [\because [Sb]_{Sol} << [Sn]_{Sol}] \qquad (1)$$

Analytical Grade Stannous chloride ($SnCl_2.2H_2O$), Antimony Chloride ($SbCl_3$), and Thioacetamide (CH_3CSNH_2) were used. The substrates used in the deposition process were Corning 7059 model glass slides. Glass slides were cleaned adopting the following procedure. Initially, the glass slides were cleaned with soap water and thoroughly rinsed with deionised water. After drying these slides, they were soaked in Potassium dichromate solution for about 24 hours. Then these slides were carefully taken out of the beaker and rinsed with deionised water. Then the slides were allowed to dry on both sides. Then these dried slides were immersed in Methanol collected in a suitable beaker. This beaker was then placed in an Ultrasonicator and Ultrasonic agitation was done for about 5 minutes. Then the slides were taken out of the beaker and both the surfaces were dried using hot air gun. These cleaned, soaked, ultrasonically agitated and dried slides were then mounted on substrate holder.

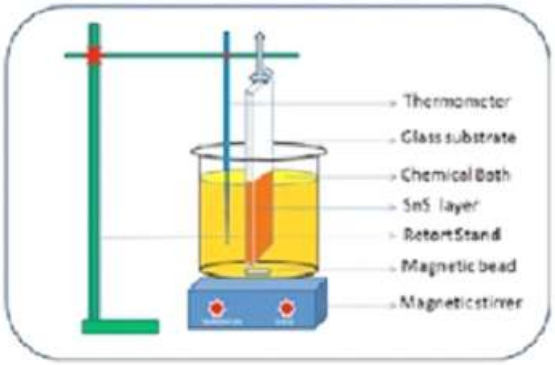

Fig 1 Experimental setup for CBD

The deposition of Sb-doped SnS thin films on the glass substrates was done using the experimental setup as illustrated in the figure 1. 1.13 gm of $SnCl_2.2H_2O$ was added to 5 ml of Acetone. The mixture was placed on a magnetic stirrer. After the solute was completely dissolved in Acetone, 15 ml of Tri Ethanol Amine (TEA) was added to the solution. Another 3 – 4 ml of Acetone was added to the solution to reduce the turbidity. Then the stirring process was continued for about 5 minutes. 0.375 gm of Thioacetamide was

added to 10 ml of deionised water in a beaker and stirred for 2 minutes. This solution was added to Stannous Chloride, Acetone and TEA solution. While continuing the stirring process, 8ml of NH_3 buffer was added to the solution. The required amount of deionised water was poured into the bath to make up the solution to 50 ml. As soon as the water was poured, the solution started slowly turning to Pale yellow and then dark brown in colour. Suitable amount of Antimony chloride was added to obtain the doping levels of 0 – 5 at%. The bath temperature was set to 70^0C. The glass substrates that were thoroughly cleaned as per the process mentioned in the beginning of this sub-section were vertically immersed into the reaction bath. The stirring was continued till 135 minutes. After the completion of the deposition process, the glass slides were slowly and carefully removed from the reaction bath and were gently rinsed with deionised water. These glass slides were allowed to dry.

2.2 Characterization

The undoped and Sb-doped SnS thin films prepared as mentioned in the previous sub section were analysed using the necessary characterisation techniques. The VG Multilab 2000 model X-ray photoelectron spectrometer with the excitation source as Al Kα radiation (1486.6 eV) was used to confirm the presence of Antimony dopant. Seifert3003TT X-ray diffractometer with Cu Kα radiation (λ = 1.542 Å) was employed to verify the crystal structure. The measurement of optical properties was done using Perkin Elmer Lambda 950 model UV-VIS-NIR spectrometer. Finally, ECOPIA HMS -3000VER Hall measurement system was employed to study the resistivity and other relevant electrical properties of the as-grown thin films.

2.3 Growth mechanism

Controlled release of Sn^{2+} and S^{2-} ions in the solution will support fruitful condensation of these ions on the aptly mounted substrates by ion – by – ion process. The ionic product of Sn^{2+} and S^{2-} must exceed the solubility product of SnS, for the effective deposition of SnS thin films. Various complexing agents like Tartaric acid, TEA etc help in proper deposition of SnS thin films by slowly releasing Sn^{2+} ions and maintaining soluble species of Sn^{2+} in aqueous medium. TEA was employed as complexing agent in this deposition process. Classical nucleation theory is used here to describe the possible growth mechanism.

$$CH_3CSNH_2 + H_2O \leftrightarrow CH_3CONH_2 + H_2S \quad (2)$$

$$H_2S + H_2O \leftrightarrow H_3O^+ + HS^- \ (K_0 = 10^{-7}) \quad (3)$$

$$HS^- + H_2O \leftrightarrow H_3O^+ + S^{-2} \ (K_1 = 10^{-17}) \quad (4)$$

Tri Ethanol Amine (TEA) represented as (T) in the following chemical equations helps in complexing Sn^{2+} ions from the Sn precursor and Sb^{3+} ions from the Sb dopant.

$$SnCl_2 + T \leftrightarrow [Sn(T)]^{+2} + Cl^- \quad (5)$$

$$SbCl_3 + T \leftrightarrow [Sb(T)]^{+3} + Cl^- \quad (6)$$

$$[Sb(T)]^{+3} \leftrightarrow Sb^{+3} + T \quad (7)$$

This complexing process helped in slow and fully controlled release of the free Sn^{2+} ions. The hydrolysis of thioacetamide resulted in S^{2-} which then combined with the free Sn^{2+} to form SnS.

$[Sn(T)]^{+2} + S^{-2} \rightarrow SnS + T$ ($K_{sp} = 1 \text{ X } 10^{-26}$ at 25^0C) (8)

3 Results and discussion

3.1 XPS analysis

The global scan XPS spectra of both the undoped (0 at%) besides Sb-doped SnS thin films in the binding energy range of (0 – 1000) eV is as shown in figure 2. The reflections in the XPS spectrum were calibrated to the carbon C 1s peak (284.6 eV). The XPS spectra of undoped SnS

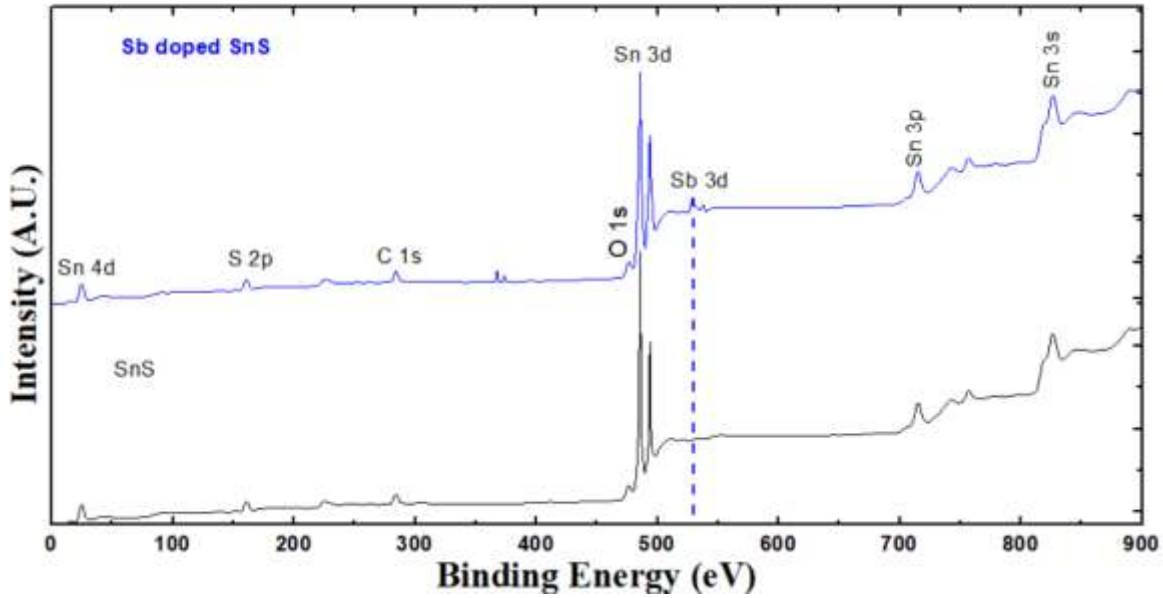

Fig 2 Global scan XPS spectra of undoped and Sb-doped SnS thin films

thin films illustrated peaks from different elements like Sn 4d, Sn 3s, S 2p, Sn 3p, C 1s, O1s, and double Sn 3d. Similar peaks were observed in the scan of the Sb-doped SnS thin films, besides double 3d peak of Sb. Presence of Sb in the films was confirmed by this Sb 3d peak. The C 1s peak belonged to the contaminants on the surface of the film. O 1s is yet another peak belonged to such contaminants. Apart from these, no other peak representing any other contaminant was present in the XPS spectra [21,31].

3.2 Structural properties

SnS thin films were grown, doped with Antimony for different [Sb/Sn] concentrations at the bath temperature $T_b = 70^0C$. The corresponding XRD patterns are illustrated in the figure 3 which hinted at orthorhombic structure with polycrystalline nature. XRD peaks were observed at 31.530^0, 30.665^0, 27.441^0 and 26.076^0 respectively in the case of both undoped and Antimony doped thin films. These peaks correspond to (111), (301), (021) and (012) planes of SnS, with (111) being the preferred orientation, in confirmation with the standard values reported in the JCPDS data 39-0354 [2,25]. At lower doping concentrations of about 1 at%, the structural properties of both undoped and Sb-doped SnS thin films are alike. The reasons may be that either the Sb atoms might have accommodated themselves in the Van der waals gaps between Sulphur and Tin atomic layers [26] or the Sb atoms might have been absorbed by grain boundaries which would not have caused any considerable structure distortion [27].

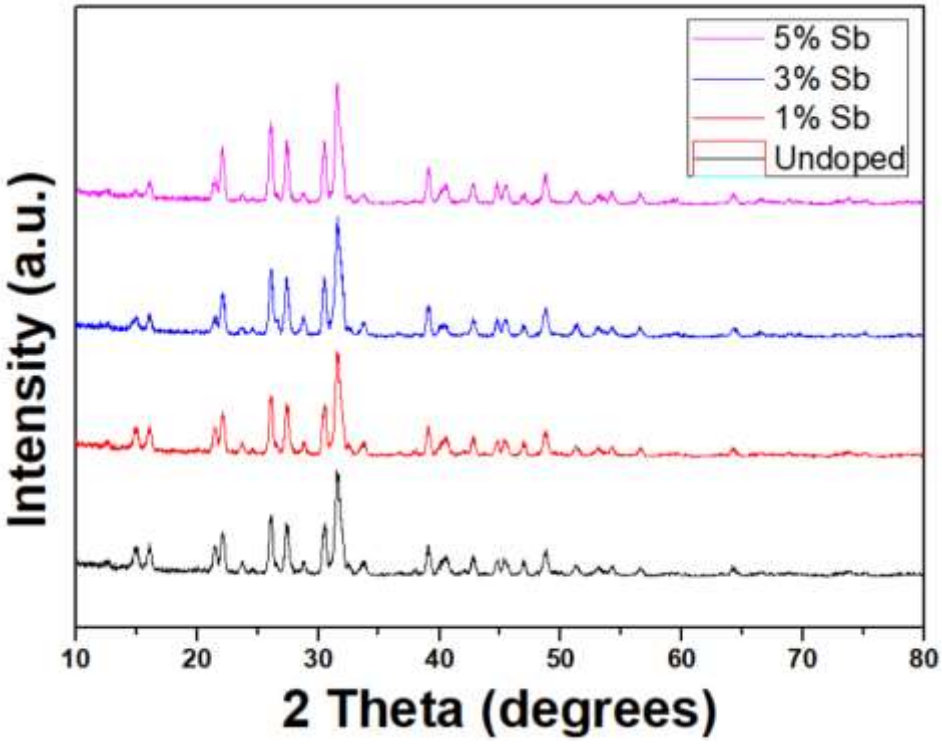

Fig 3 XRD patterns of pristine and Sb-doped (1%, 3% and 5%) thin films

Sharper and more intense Bragg peaks were observed with the Sb-doping concentration increasing from 0% to 5% which pointed at significant improvement in crystallinity. Sb-atoms might have benefitted the growth of SnS films, with the formation of new nucleation centres [28].

3.3 Optical properties

It was clear from the figure 4(a) that the absorption coefficient (α) was in the order of $> 10^6$ cm^{-1} for the as-grown films. It was observed that the absorption edge slightly shifted to higher wavelength region as the doping concentration was increased. The obvious consequence of this shift was the decrease of optical band gap. The following relation was employed in evaluating the energy band gap of the semiconductor films[29]

$$(\alpha h\nu)^{1/n} = A(h\nu - E_g) \qquad (9)$$

where the band edge constant is denoted by (A) while direct transition band gap is represented by (E_g). The SnS is considered as more suitable for direct band gap material and hence n = ½ [30]. Figure 4b shows the plot between $(\alpha h\nu)^2$ vs Photon energy for undoped and antimony doped SnS thin films. The (E_g) was determined by the extrapolation of the linear portions of the curve to reach the x-axis as α=0. The optical band gap thus determined for the pristine SnS thin films was 1.25 eV while that in the case of antimony doped SnS thin films were 1.194 eV for 1% doping, 1.18 eV for 3% doping and 1.147 eV for 5% doping. Presence of Sb in the SnS lattice was the key reason for the reduction in the optical band gap [29].

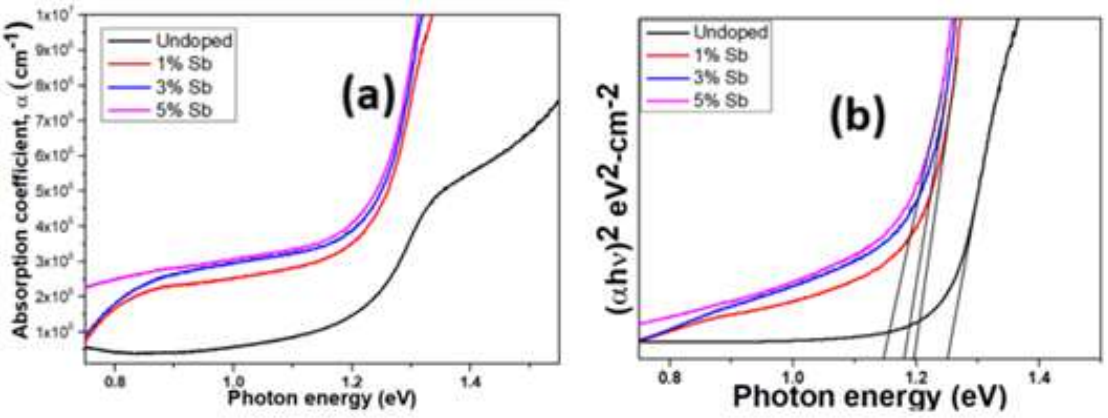

Fig 4(a) Absorption coefficient (b) $(\alpha h\nu)^2$ Vs Photon energy ($h\nu$) of undoped and Sb-doped (1%, 3% and 5%) SnS thin films.

3.4 Electrical properties

Table 1 lists out the various electrical parameters like resistivity, carrier concentration and Hall mobility for the undoped and Sb-doped (1%, 3% and 5%) SnS thin films. The resistivity of the these thin films decreased with the rise in the doping concentration of Sb which might be owing to the replacement of Sn^{2+} by the Sb^{3+} ions which resulted in the increase in the conductivity. From the table 1, the lowest resistivity of 2.72 x 10^{-2} Ω - cm was observed in the case of 5% Sb-doped SnS thin film which represented the better crystallinity. This was confirmed in figure 1 also. Further, it was observed that doping Sb not only increased the carrier concentration but also improved the Hall mobility. Similar observations were reported in the case of Ag doped SnS thin films [16].

Sample	$\boldsymbol{Resistivity\ (\Omega - cm)}$	$\boldsymbol{Carrier\ Concentration\ (cm^{-3})}$	$\boldsymbol{Hall\ mobility\ (cm^2/V-S)}$
Undoped	6.02 x 10^{2}	5.74 x 10^{15}	140.23
1% Sb-doped	5.96 x 10^{1}	1.18 x 10^{17}	392.46
3% Sb-doped	3.54 x 10^{-1}	3.96 x 10^{18}	506.62
5 % Sb-doped	2.72 x 10^{-2}	3.65 x 10^{19}	665.36

4 Conclusions

Sb-doped SnS thin films were deposited along with the undoped films using CBD. The properties like structural, optical and electrical are studied and reported in this paper. The existence of Antimony dopant in the SnS thin films was confirmed from the XPS studies. Improved crystallinity was observed in the case of 5% Antimony doped SnS thin films compared to the pristine, 1% and 3% Antimony-doped SnS thin films. Further, doping SnS with Antimony, reduced the optical band gaps with about 1.147 eV band gap for 5% Sb-doped SnS thin film. Also, the electrical properties were greatly influenced by the Sb-doping with lowest resistivity, highest hall mobility and highest carrier concentration recorded for 5% Antimony doped SnS thin films. These observations suggest the appropriateness of Sb-doped SnS thin films in the case of photovoltaic applications.

References:

1. J.J. Loferski, Theoretical considerations governing the choice of the optimum semiconductor for photovoltaic solar energy conversion, J. Appl. Phys. 27 (1956) 777–784.
2. C. Chen, C. Huang, Effects of silver doping on electromigration of eutectic SnBi solder, J. Alloy. Compd. 461 (2008) 235–241.
3. P. Sinsermsuksakul, L. Sun, S.W. Lee, H.H. Park, S.B. Kim, C. Yang, et al., Overcoming efficiency limitations of SnS-based solar cells, Adv. Energy Mater. 4 (2014) 1–7.
4. A. Niemegeers, M. Burgelman, A. De Vos, On the CdS/CuInSe2 conduction band discontinuity, Appl. Phys. Lett. 67 (1995) 843–845.
5. T. Minemoto, T. Matsui, H. Takakura, Y. Hamakawa, T. Negami, Y. Hashimoto, T. Uenoyama, M. Kitagawa, Theoretical analysis of the effect of conduction band offset of window/CIS layers on performance of CIS solar cells using device simulation, Sol. Energy Mater. Sol. Cells 67 (2001) 83–88.
6. L. Sun, R. Haight, P. Sinsermsuksakul, S. Bok Kim, H.H. Park, R.G. Gordon, Band alignment of SnS/Zn(O, S) heterojunctions in SnS thin film solar cells, Appl. Phys. Lett. 103 (2013) 1–5.
7. P. Malkeshkumar, R. Abhijit, Magnetron sputtered Cu doped SnS thin films for improved photoelectrochemical and heterojunction solar cells, RSC Adv. 4 (2014) 39343–39350.
8. M. Reghima, A. Akkari, C. Guasch, N. Kamoun-Turki, Effect of indium doping on physical properties of nanocrystallized SnS zinc blend thin films grown by chemical bath deposition, Renew. Sustain. Energy 4 (1–12) (2012) 011602.
9. W. Huang, S. Cheng, H. Zhou, Electrical and optical properties of In-doped SnS thin films prepared by thermal evaporation, ECS Trans. 44 (2012) 1295–1301.
10. V.F. Gremenok, V.Y. Rud, Y.V. Rud, S.A. Bashkirov, V.A. Ivanov, Photosensitive thin-film In/p-PbxSn1−xS Schottky barriers: fabrication and properties, Semiconductors 45 (2011) 1053–1058.
11. S. Zhang, S.Y. Cheng, H.J. Jia, H.F. Zhou, Preparation and characterization of aluminium-doped SnS thin films, Adv. Mater. Res. Trans. Tech. Publ. 418 (2012) 712–716.
12. A. Dussan, F. Mesa, G. Gordillo, Effect of substitution of Sn for Bi on structural and electrical transport properties of SnS thin films, J. Mater. Sci. 45 (2010) 2403–2407.
13. M. Devika, N.K. Reddy, K. Ramesh, K.R. Gunasekhar, E.S.R. Gopal, K.T.R. Reddy, Low resistive micrometer-thick SnS:Ag films for optoelectronic applications, J. Electrochem. Soc. 153 (2006) G727–G733.
14. K. Santhosh Kumar, A.G. Manohari, S. Dhanapandian, T. Mahalingam, Physical properties of spray pyrolyzed Ag-doped SnS thin films for opto-electronic applications, Mater. Lett. 131 (2014) 167–170.
15. M. Reghima, A. Akkari, C. Guasch, N. Kamoun-Turki, Structural, optical, and electrical properties of SnS:Ag thin films, J. Electron. Mater. 44 (2015) 4392–4399.

16. Sreedevi Gedi, Vasudeva Reddy Minnam Reddy, Tulasi Ramakrishna Reddy Kotte, Soo-Hyun Kim, Chan-Wook Jeon, Chemically synthesized Ag-doped SnS films for PV applications, Ceramics International 42 (2016) 19027 – 19035.
17. C. Lilia, C. Triana, P.B.G. Gordillo, Preparation and characterization of SnS:Bi thin films, Braz. J. Phys. 41 (2011) 15–20.
18. P. Sinsermsuksakul, R. Chakraborty, S.B. Kim, S.M. Heald, T. Buonassisi, R.G. Gordon, Antimony-doped tin(II) sulfide thin films, Chem. Mater. 24 (2012) 4556–4562.
19. Y. Yongli, C. Shuying, Preparation of SnS∶Ag thin films by pulse electrodeposition, J. Semicond. 4177 (2008) 1–5.
20. M. Kilani, B. Yahmadi, T. Kamoun, M. Castagne, Effect of Al doping and deposition runs on structural and optical properties of In2S3 thin films grown by CBD, J. Mater. Sci. 46 (2011) 6293–6300.
21. S. Cheng, G. Conibeer, Physical properties of very thin SnS films deposited by thermal evaporation, Thin Solid Films 520 (2011) 837–841.
22. M. Vasudeva Reddy, P. Babu, K.T. Ramakrishna Reddy, R.W. Miles, X-ray photoelectron spectroscopy and X-ray diffraction studies on tin sulfide films grown by sulfurization process, J. Renew. Sustain. Energy 5 (2013) 1–6.
23. M. Vasudeva Reddy, G. Sreedevi, P. Chinho, R.W. Miles, K.T. Ramakrishna Reddy, Development of sulphurized SnS thin film solar cells, Curr. Appl. Phys. 15 (2015) 588–598.
24. http://www.xpsfitting.com/2017/10/antimony.html
25. M. Vasudeva Reddy, G. Sreedevi, P. Babu, Z. Guillaume, K.T. Ramakrishna Reddy, P. Chinho, Influence of different substrates on the properties, Sci. Adv. Mater. 7 (2015) 1–5.
26. T.H. Patel, R. Vaidya, S.G. Patel, Growth and transport properties of tin monosulphoselenide single crystals, J. Cryst. Growth 253 (2003) 52–58.
27. I. Lefebvre-Devos, J. Olivier-Fourcade, Lithium insertion mechanism in SnS2, Phys. Rev. B 61 (2000) 3110–3116.
28. J. Morales, E. Andrade, M. Miki-Yoshida, Influence of Al, In, Cu, Fe and Sn dopants in the microstructure of zinc oxide thin films obtained by spray pyrolysis, Thin Solid Films 366 (2000) 16–27.
29. Kumar, AG., Sarmash, T.S., Obulapathi, L. Rani, D.J., Rao, T.S., Asokan, K., Structural, optical and electrical properties of heavy ion irradiated CdZnO thin films, Thin Solid Films., 605 2016: pp.102–107. https://doi.org/10.1016/j.tsf.2015.12.024.
30. Rani, D.J., Kumar, A.G.S., Obulapathi, L., Rao, T.S., Dielectric and optical properties of zirconium titanate thin films by reactive DC magnetron co-sputtering, IEEE Trans. Dielectr. Electr. Insul., 26 2019: pp.1134–1138. https://doi.org/10.1109/TDEI.2019.007887
31. Guru Sampath Kumar ANKISETTY, Vijay Kumar JINDE, Mahesh Kumar UNGARALA, Siva Kumar PENDYALA, Obulapathi LAVULURI, Sharon Samyuktha VADDE, Microwave Assisted Sintering of Sr-doped Zinc Titanate (Sr0.2Zn0.8TiO3) Nano-ceramics, MATERIALS SCIENCE (MEDŽIAGOTYRA). Vol. 29, No. 4. 2023. http://doi.org/10.5755/j02.ms.33625